Impact of Burnished and Brushed Surface Preparation on Gold Bond Pads: Bond Strength and Wire Bond Quality in Microelectronics

Matteo Forgione, P.E.
Forgione Engineering, Inc.
160 Tanner St.
Lowell, MA 01852, USA
Ph: 844-632-4364; Fax: 844-632-4364
Email: matteo@forgioneengineering.com

Abstract

Wire bond strength depends on various factors beyond material selection, bonding machinery, and operational parameters. This study investigates how surface roughness of gold bond pads on a 99.6% Alumina Ceramic, TaN, TiW, Au plating stack affects bonding. Pads were solvent and argon plasma cleaned to reduce effects from residual contamination. Two mechanical surface preparations, burnishing and brushing, were compared to an unmodified control. While water contact angle, an indicator of possible surface contamination, was measured across all samples, it showed no statistically significant correlation with bond performance, suggesting cleanliness was not a limiting factor. Bonds were formed using 0.001" DIA 99.99% Au wire via the Crescent on Ball (COB) method, with nine bonds fabricated per test condition. Bond strength was evaluated using industry standards EIA/JESD22-B116 – Wire Bond Shear Test Method and MIL-STD-883E – Method 2011 Destructive Bond Pull. Destructive shear tests revealed a statistically significant improvement in bond strength with burnishing surface preparation: burnished bonds averaged 48.4 gf, brushed 40.4 gf, and control 34.5 gf. In one-tailed analysis, burnished pads yielded a Z-score of 1.853 ($p = 0.032$) against the control group, confirming statistical significance. Pull strength was unaffected by surface preparation, with 24 of 27 bonds breaking at the neckdown and 3 at the heel, ranging from 1.505 to 5.930 gf, with minimal mean variation and variance across groups. These results, along with water contact angle observations and surface imaging and roughness measurements of bonded surfaces, underscore that mechanical surface preparation —especially burnishing — can lead to statistically significant improvements in wire bond ball-shear test results, offering a practical path to reducing bond failures in high-reliability electronics.

Key words

Wire Bonding, Wire, Microelectronics, Contamination, Integrated circuit interconnections, Gold.

I. Introduction

Wire bonding is a key interconnection method for microelectronics, and the reliability of these connections is highly dependent on the integrity of the wire-to-substrate bond. Microelectronics manufacturers typically rely solely on solvent and plasma cleaning of substrates, Integrated Circuits (ICs), and electrical components. However, the potential role of mechanical surface preparation in enhancing bond strength remains underexplored. Further research is necessary to better understand its impact and to determine whether it can contribute meaningfully to bond reliability in high-performance applications.

There are a number of research papers focusing on different cleaning methods for surface preparation. Kidd emphasizes the importance of surface-sensitive cleaning processes for maintaining long-term bond reliability. Their work in microelectronics assembly highlighted how trace surface contamination, oxide growth, and inconsistent cleaning protocols can introduce bond failures—even when mechanical attachment appears sufficient. By optimizing plasma conditions and post-cleaning storage environments, they achieved improved process stability and joint integrity [1]. Jackson evaluated a CO2 Snow Spray cleaning method versus standard solvent/plasma cleaning using solvents such as Acetone before Au ribbon bonding (0.005” x 0.007”). The CO2 approach removed contaminants such as tape adhesive, finger oils, flux, and silicone gel effectively, with bond pull strengths similar to conventional cleaning—though the focus was solely contamination control, not mechanical pad texture or roughness [2]. Alberici showed that plasma and sputter cleaning substantially restore bonding performance and reliability after removing dry-etch fluorine residues, which can crystallize, and oxide from aluminum pads that can significantly degrade bonding performance [3]. Similarly, Chan demonstrated improved bond performance on both rigid and flexible substrates when plasma-treated surfaces were used instead of untreated ones [4].

Various research has pointed towards material characteristics and surface properties affecting bond performance. Two reviews [5][6] discuss material related factors on quality and reliability in performance when using Au, Cu, and Al wire bonding used in the microelectronics, yet they largely omit discussion of any surface properties of the substrates in the wire bonded products. Guenther further found that pad morphology—including spikes and roughness on laser-direct-structured and high-frequency PCB substrates—directly reduces wire bonding consistency and strength, reinforcing that surface characteristics must be finely controlled to achieve reliable bonds [7]. Another comprehensive review by Zulkifli examined microstructural changes at the intermetallic bond level and their impact on reliability but did not address the effects of surface preparation, such as hardening or softening of the ball or bond pads, using mechanical pad treatments as a contributing factor to bond strength [8]. Chen investigated the post-bonding sulfidation behavior of palladium-coated copper wire with a flash-gold layer, highlighting how surface conditions can deteriorate over time if not properly stabilized—a key consideration for surface-prepped pads exposed to environmental factors [9]. Fan further confirmed that Pd-layer thickness and substrate condition play crucial roles in bonding reliability, emphasizing that even micro-level surface variations can impact intermetallic formation and joint strength [10]. A study for EV power module terminals by Kim evaluated how different surface finishes (bare Cu, electroless Ag, and electroless Ni-immersion Au) on ceramic substrates and bonding methods (reflow soldering and ultrasonic welding) affect terminal joint–substrate reliability. They found that during reflow soldering, interfacial intermetallic compound (IMC) layer composition and morphology of the reflow-solder joints varies with surface finish — and thus shear strength at the terminal joints depends strongly on pad metallization. Results indicated that bare Cu substrate had greater dynamic recrystallization than other substrates after ultra-sonic welding. But, no significant differences in morphology versus surface finish were found for the ultrasonic-welded joints [11].

Burnishing is a controversial procedure, with literature containing both supportive and critical perspectives on its effectiveness. A study highlighted by George Harman in *Wire Bonding in Microelectronics* focused on Aluminum (Al) wedge bonds on a Gold–Nickel–Copper (Au–Ni–Cu) Printed Circuit Board (PCB) plating stack revealed failures after up to 1,000 thermal cycles between 0–125 °C, concluding that “the rougher the surface, the more likely the bonds will be weak” [12]. Those studies referenced in Harman’s foundational text were conducted in the early to mid-1980s and appear to center on thick-film hybrid metallization; the original data remains inaccessible. Harman also further theorizes that mechanical scouring tools may introduce particles or FOD (foreign-object debris), posing a contamination risk and potentially reducing wire bondability [12]. However, controlled burnishing practices can avoid FOD generation and remain compatible with microelectronics assembly standards.

Despite growing research on wire bonding tools, process parameters, and wire materials, examination of mechanical surface preparation remains limited. Therefore, this study aims to isolate and identify the significance of mechanical surface preparation on the strength of wire bonds while using industry standard solvent and plasma cleaning techniques. Measurements of surface roughness and average water contact angle were recorded to verify progressive increase in readiness to bond, ensuring that the mechanical surface preparations were isolated in the experiment. This information may aid in predicting bond strength and the ability to meet pull-strength requirements (3 gf) and destructive ball-shear test requirements (21.1 gf). Bond testing equipment is used to measure both pull and ball-shear strength.

II. Experimental and Evaluation

Materials and Equipment:

- Ceramic substrate with 99.6% Alumina Ceramic, 0.015" thick with TaN, TiW, Au plating stack, 100-15µin thickness gold surface polished to 1µin Max.
- Gold wire, AMETEK 549001-1, 0.001" (1 MIL) DIA 99.99% AU
- BTG Surface Analyst Model SA3001
- BTG Water Cartridge 11118
- BTG Calibration Card 11363V40
- Fixture for SA3001, FUS-230817001-01-A
- Nordson March AP 600Plasma cleaner
- Acetone
- Isopropanol (99% IPA)
- Micro Burnishing tool – Forgione FUS-180117001-09-A – 0.004” radius TiN Coated
- Micro Brush, FUS-241202001-02-A, 0.006” carbon steel bristles
- Keyence VHX-S660E
- Keyence VK-X3000
- Palomar Wire Bonder, Model 8000
- DAGE Bond Tester, Model 4000 TPAXY, with WP100 for pull testing, BS100 for shear testing.
- Leica M80 Stereo Microscope

Methods/Sample Preparation:

Substrate layout:

A single 99.6% Alumina Ceramic substrate with a TaN, TiW, Au (polished to 1 microinch max) plating stack was used to create 3 sets of 6 bond pads, laser marked to clearly define the 0.2" in diameter bond pads by column and row as seen in Fig. 1.

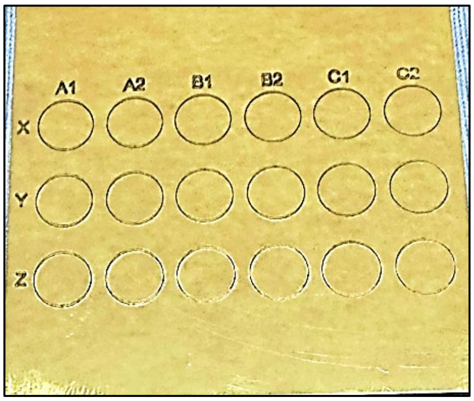

Fig. 1 – TaN, TiW, Au Plated Ceramic Substrate Laser Marked

The large diameter of .2" accommodated the droplet size dispensed by the BTG-3001 surface analyst, and to allow for multiple bonds per pad. Each set of bond pads become a unique configuration based on the cleaning and surface preparation methods used before wire bonding seen in Table 1.

Table 1 – Configurations/Preparation Methods

Polished Solvent/Plasma Cleaned	Polished Solvent/Plasma Cleaned BURNISHED	Polished Solvent/Plasma Cleaned BRUSHED
XA-P	XB-P	XC-P
YA-P	YB-P	YC-P
ZA-P	ZB-P	ZC-P

Configurations:

Three configurations are designated: The control group (A-Columns), burnished group (B-Columns), brushed group (C-Columns), and three rows for each group. Individual bond pad locations are defined by Row x Column, for example XA1 is the top-left bond pad. Wire bond loops are made between Sub Columns 1 and 2, for each set (A,B,C), on each row (X,Y,Z), for example the first loops are between XA1 and XA2. The second column is reserved for shear tests where the ball is made for the star of the interconnecting bond. The bond pad designations can be seen in Fig. 2.

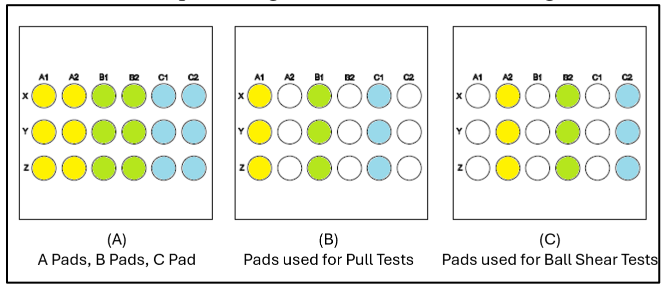

Fig. 2 – Bond Pad Layout on Substrate

Using the prepared sample which contains all bond pads, three sets of 6 bonds (3 loops) were made for each configuration allowing for pull-testing of 9 wire bonds and ball-shear testing of 9 bonds for each preparation method, where the control configuration is shown in Fig. 3. Note that any bonds in column A were pull tested, and those in column B shear tested.

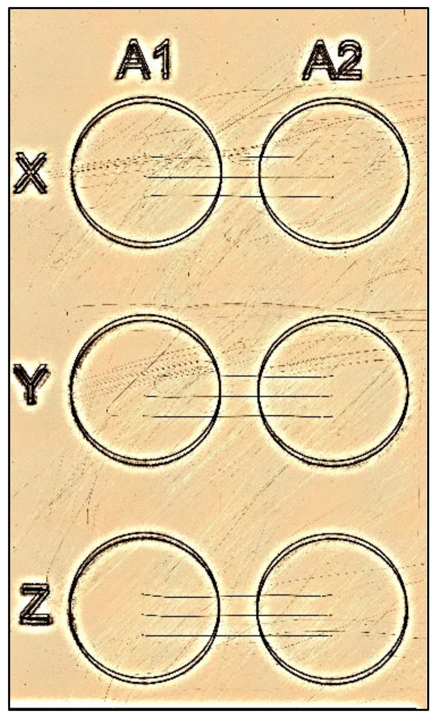

Fig. 3 - Control Configuration Showing 9 loops, 18 bonds

For all bond pad groups, acetone and isopropanol were used for preliminary cleaning. Brushing and burnishing tools were cleaned using the same, and mechanical surface preparation was performed under magnification using a Leica M80 stereo microscope. Plasma cleaning was performed on all bond pad groups using the following parameters: Argon, 300 mTORR, 300 W, 600 seconds, 5VDC Bias, BP/RP 135). Images of the substrate, wire bonds, and ball-shear results were captured with a Keyence VHX S660E. Wire bonding was performed using the

Crescent on Ball (COB) technique (Method 2017). Bonds loops are made between pads parallel to the row, for example row X gets a loop bonded between A1 and A2, therefore XA1 to XA2. The same scheme is used throughout the study. Three loops are made on each set of pads. Before bonding, the tip created a pre-ball on pad 1, then moves to create a ball on pad 2, then the loop is created, and the stitch is made on top of the pre-ball on pad 1. A total of 3 loops on 6 sets of pads yielded 27 loops, and 54 bonds.

Characterization Techniques: The methods of characterization were EIA/JESD22-B116, Wire Bond Shear Test Method and MIL-STD-883L, Method 2011, Destructive Bond Pull.

The following detailed experimental procedure was followed to generate the final configured bond pads for the wire bonding and performance testing process.

Experiment Procedure:

1.) Assign Configurations:
   Config A - Solvent cleaned, plasma cleaned (6 pads)
   Config B - Solvent cleaned, burnished, plasma cleaned (6 pads)
   Config C - Solvent cleaned, brushed, plasma cleaned (6 pads)
2.) Before any cleaning or preparation, surface imaging and surface energy are measured using BTG-3001.
3.) Clean all bond pads and surrounding areas with acetone using a natural hair acid brush for a minimum of 10 seconds.
4.) Rinse all bond pads and surrounding areas with acetone for a minimum of 10 seconds, and then 99% IPA (Isopropanol) for a minimum of 10 seconds.
5.) Repeat steps 1 and 2 to clean the burnishing tool and the brush tool in preparation for use.
6.) Measure average water contact angle of all bond pads using BTG-3001.
7.) Surface preparation by configuration:
   Config A - No surface preparation required after solvent cleaning
   Config B - Burnished – Under magnification, using the 0.002" radius TiN coated burnishing), manually burnish the surface of the bond pads in one direction until the entire surface is uniform and no further change is seen to the surface; ensure the finish matches when compared to the other bond pads being burnished.
   Config C - Brushed - Under magnification, using the 0.006" carbon steel wire brush (flat bristle pattern), manually brush the surface of the bond pads in one direction until the entire surface is uniform and no further change is seen to the surface; ensure the finish matches when compared to the other bond pads being brushed.
   Schematic views of the burnishing tool and brush are shown in Fig. 4.
8.) Measure average water contact angle of all bond pads using BTG-3001 Analyst.
9.) Plasma-clean the sample and all bond pads.
10.) Measure average water contact angle of all bond pads using BTG-3001 Analyst
11.) Protect samples from contaminants by packaging until bonding is imminent.
12.) Capture magnified images of surfaces
13.) Capture surface roughness measurement
14.) Wire bond all samples
15.) Test 3 sets of 3 bonds for each preparation method (Columns A1, B1, C2) using MIL-STD-883L, Method 2011, Destructive Bond Pull
16.) Test 3 sets of 3 bonds for each preparation method (Columns A2, B2, C2) using EIA/JESD22-B116, Wire Bond Shear Test Method.
17.) Surface roughness for all bond pads was measured by the Keyence VK-X3000

The Micro Burnishing Tool and Micro Wire Brush Tool made by Forgione Engineering depicted in Fig. 4 were used for the burnished and brushed pads, respectively.

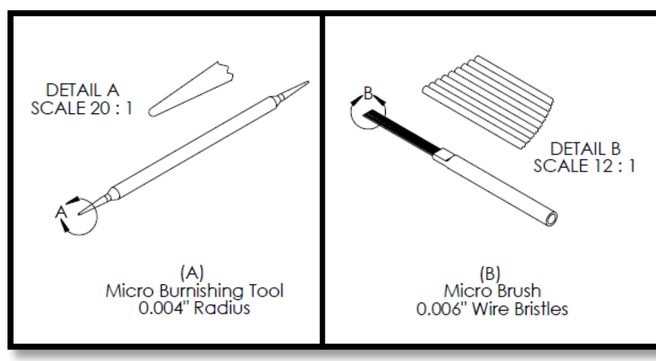

Fig. 4 – (a) Micro Burnishing Tool, and (b) Micro Wire Brush

An image captured showing wire bonds and the loops between two pads is shown in Fig. 5.

Fig. 5 - Wire Bonds and Loops Location YB, Burnished Pads

III. Results and Discussion

Section 1: Average water contact angle was observed changing as each cleaning or preparation process was performed. The final water contact angles for all methods ranged from 31.1 to 40.1 degrees, as shown in Fig. 6, with the highest value associated with burnished, which would typically be an indicator of poorer performance for an adhesive bond, and lowest, brushed; however the strength results show the inverse, and the lack of intuitive correlation to average water contact angle to the wire bond quality, when modified by mechanical surface finish, meaning that these data simply provide confirmation that the sample has been adequately cleaned within the context of the scope of the experiment. The differences of average water contact angle for burnished and brushed surfaces were not statistically significant when compared to the control sample.

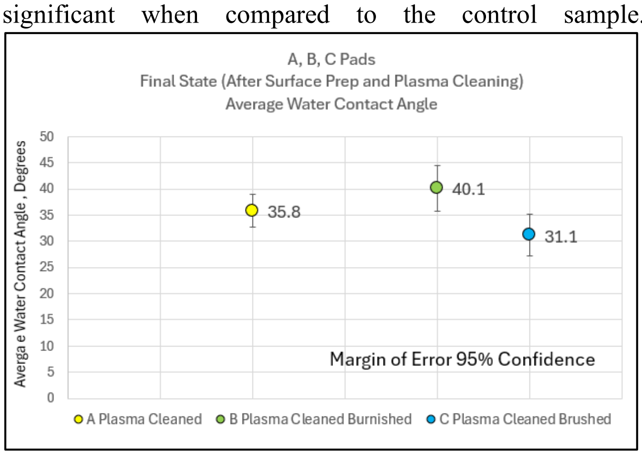

Fig. 6 - Average Water Contact Angles for All Configurations

Section 2: Wire Bond pull strengths did not appear to provide any meaningful insight into the surface preparation techniques, as the results were essentially indistinguishable from the control group. The long distance for the loops (0.313") was dictated by the large bond pads to allow for the water contact angle measurements may have contributed to necking of the wire. As shown in Fig. 7, the variability of the pull strengths and the similar mean strengths did not provide any significant insight into the bond strength itself, essentially showing wire strength. Compared to the typical non-destructive pull test load of 2.4 gf, the low destructive loads all averaging below the required 3 gf load, and mode of failure indicate that the long loop parallel to the substrate results in a higher effective load on the wire than expected, while not allowing for bond lift-off. In future work, bonds more closely spaced will eliminate this effect and isolate the effect of burnishing on pull strength generating lift-off data.

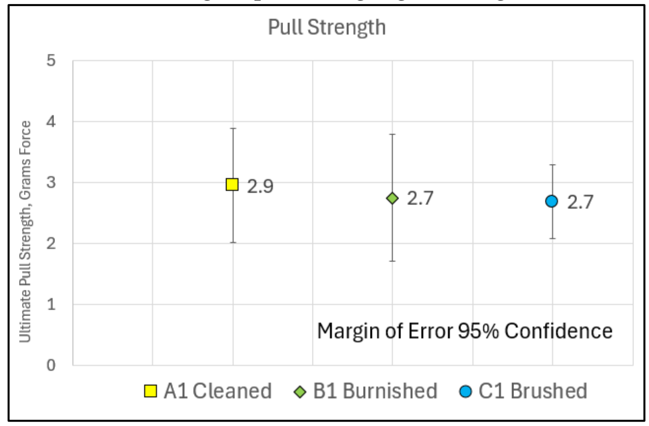

Fig. 7 - Destructive Pull Test Results for All Configurations

Section 3: Surfaces that were mechanically prepared by brushing showed some effect on ball-shear results, however not statistically significant. The very low average water contact angle of the brushed surfaces provides some insight into the possible efficacy of its use in adhesive bonding.

Burnished surfaces provided statistically significant results, as well as a smaller margin of error, suggesting that burnishing not only results in high ultimate shear test results, but lower variability. Fig. 8 shows the mean shear test results of the burnished pad wire bonds was 48.4 gf, compared to 34.5 gf for the control group, and 40.4 gf for brushed group. In the one-tailed test, the burnished pad wire bonds yielded a Z-score of 1.853 (p-value of 0.032) when compared to the control group which was simply solvent and plasma cleaned and part of the same plating stack.

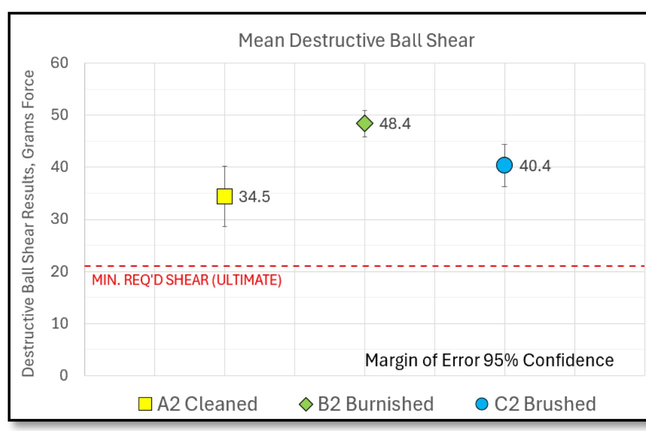

Fig. 8 - Destructive Shear Tests for All Configurations

A post-shear image of a burnished pad bond YB2 can be seen in Fig. 9 appearing relatively solid and clean.

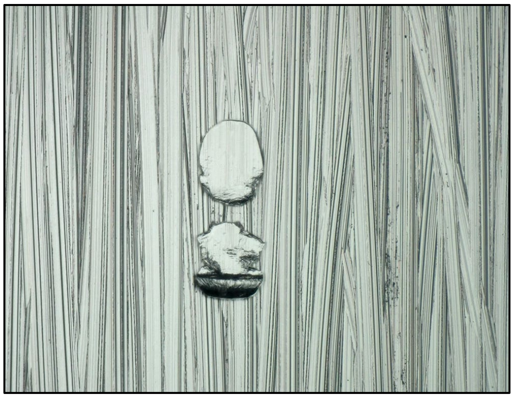

Fig. 9 – Post-Shear Image, Location YB2 (Burnished)

A post-shear image of a brushed pad bond ZC2 is shown in Fig. 10, with a rough edge, indicating the possibility that the direction of scour may have an effect at the periphery of the bond.

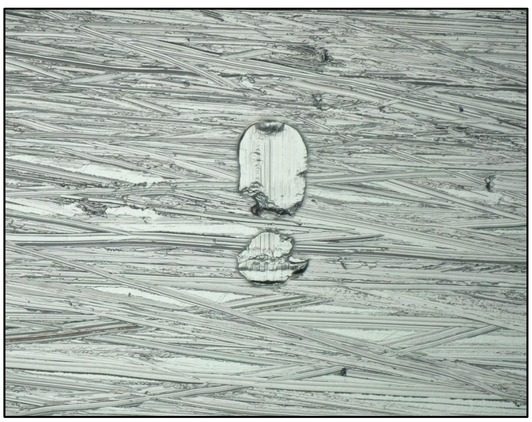

Fig. 10 - Post Shear Image Location ZC2 (Brushed)

Section 4: Average surface roughness was observed changing as each preparation process was performed. Surface roughness of the A columns, controls, were seen to have fairly uniform surface roughness with an average of 0.449 µin and average standard deviation of 0.0460 µin. The range of surface roughness observed in the B and C columns was greater. Burnishing had the highest surface roughness with the lowest standard deviation. The comparison between control, burnished, and brushed can be seen in Table 2.

Table 2 – Surface roughness and average standard deviation of control (A2), burnished (B2), and brushed (C2) surfaces

	A2	B2	C2
Average Surface Roughness (µin)	0.446	13.8	9.26
Average Standard Deviation (µin)	0.048	0.546	3.89

Shear tests were compared against surface roughness for the second columns (A2, B2, and C2). Fig. 11 shows the plotted surface roughness measurements and shear test results, suggesting that the higher roughness burnished surfaces improved bond quality. While roughness alone may not be the driver for higher shear test result, an apparent correlation exists.

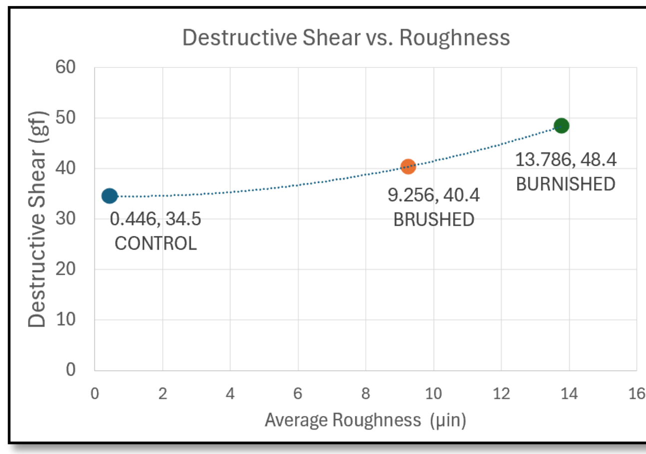

Fig. 11 – Mean Destructive Shear Force vs. Average Surface Roughness

Fig. 12 and Fig. 13 show the surface roughness of the control surface and the laser passes over the control surface, respectively. As a comparison, Fig. 14 and Fig. 16 show the surfaces of the burnished and brushed surfaces, respectively. Fig. 15 and Fig. 17 show the laser passes on the burnished and brushed surfaces, respectively**.**

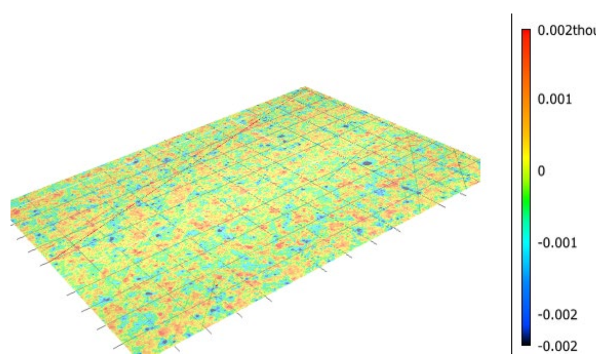

Fig. 12 – Surface Measurement diagram from Keyence VK-X3000 of the control surface (ZA2)

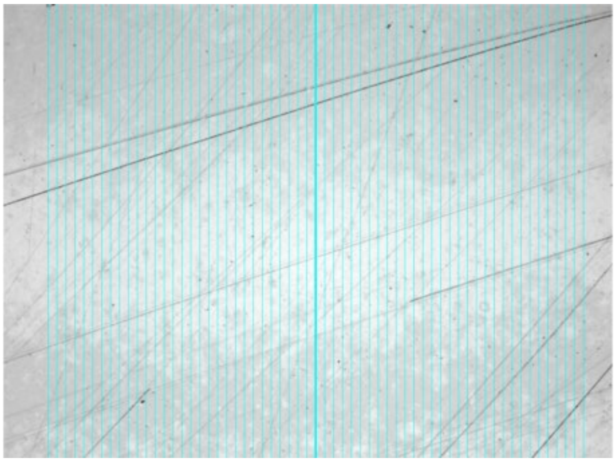

Fig. 13 – Laser passes (light blue) over control surface with Keyence VK-X3000 (ZA2)

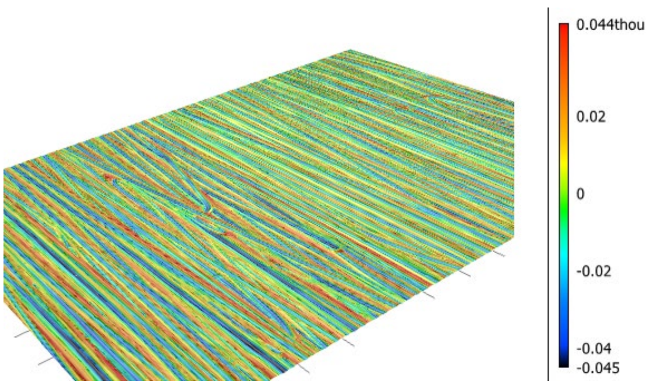

Fig. 14 – Surface Measurement diagram from Keyence VK-X3000 of the burnished surface (ZB2)

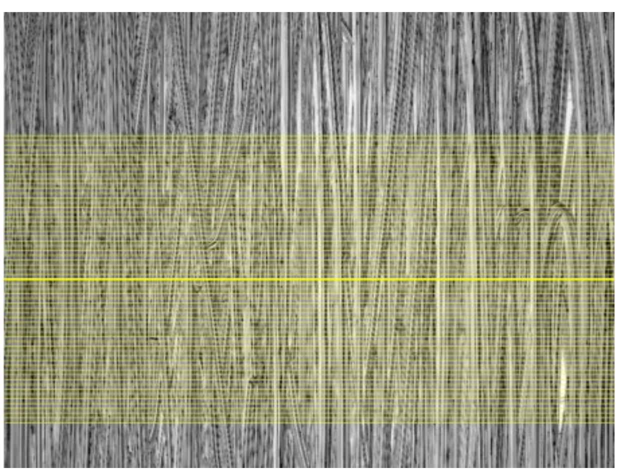

Fig. 15 – Laser passes (yellow) over burnished surface with Keyence VK-X3000 (ZB2)

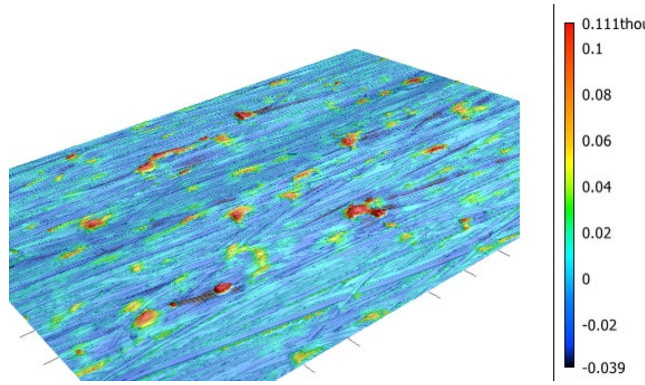

Fig. 16 – Surface Measurement diagram from Keyence VK-X3000 of the brushed surface (XC2)

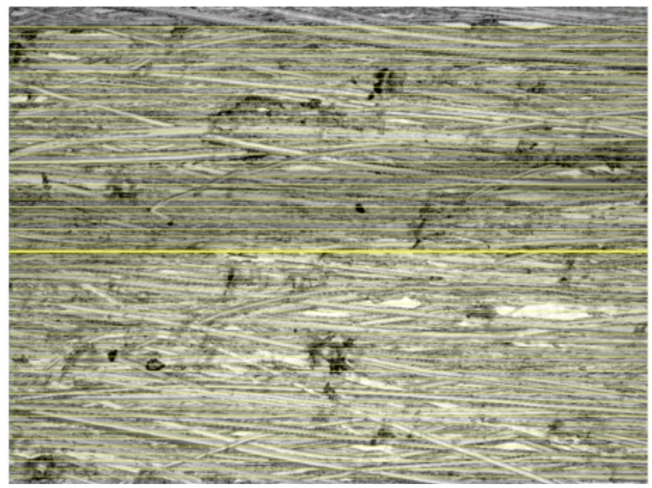

Fig. 17 – Laser passes (yellow) over brushed surface with Keyence VK-X3000 (XC2)

IV. Conclusion

The implementation of burnishing bond pads can significantly increase the reliability of interconnects in high-reliability microelectronics. This initial study alone shows a 40% increase in destructive shear test results by implementing a micro burnishing technique to mechanically prepare the gold surface before bonding and when compared to a control group on the same substrate and plating stack, the burnished surface yielded a mean destructive ball-shear test force of 48.4 gf, 78.5% greater than the 21.1 gf test load requirement. While the results show practical promise, future work including thermal cycling tests, surface hardness testing to explore different types of surface textures (peaks and valleys, mounds, long striations, randomized textures, core void volume, density of peak values, aspect ratio of surface texture, etc.), and surface analysis using Auger Electron Spectroscopy (AES) can provide insight into the underlying contributing factors that cause this increased bond strength, where the surface finish properties and metallic or intermetallic bond formation combined with the thermosonic energy can be better understood. It is expected that varying only the surface finish within a specific range and using a burnishing or scouring technique will result in the highest strength metallic bond formation and thus better wire bond reliability and performance due to an effect on microstructure and hardness of the bond.

Acknowledgment

The author would like to acknowledge Richard Rochford of BAE Systems for providing continuous opportunities for innovative and meaningful projects in the microelectronics industry, Toron Deluz of BAE Systems for assistance in performing the experimental procedure, Professors Juan Pablo Trelles and Glenn Sundberg, and Dean James Sherwood of the University of Massachusetts Lowell.

References

[1] Kidd, E. J., Campbell, B., & Dillingham, R. G. (2019). Controlling Surface Sensitive Processes in Microelectronics Manufacturing to Improve Wire Bonded Joint Reliability. *International Symposium on Microelectronics*, *2019*(1), 000515–000518. https://doi.org/10.4071/2380-4505-2019.1.000515

[2] Jackson, D. (2014). *Surface Preparation for Wire Bonding*. CleanLogix Application Note AN1001.

[3] Alberici, S., Coulon, D., Joubin, P., Mignot, Y., Oggioni, L., Petruzza, P., … Zanotti, L. (2003). Surface treatment of wire bonding metal pads. *Microelectronic Engineering*, *70*(2-4), 558–565. https://doi.org/10.1016/S0167-9317(03)00418-0

[4] Chan, Y. H., Kim, J.-K., Liu, D., Liu, P. C. K., Cheung, Y. M., & Ng, M. W. (2006). Comparative performance of gold wire bonding on rigid and flexible substrates. *Journal of Materials Science: Materials in Electronics*, *17*(8), 597–606. https://doi.org/10.1007/s10854-006-0005-4

[5] Gan, C. L., Classe, F., Chan, B. L., & Hashim, U. (2014). Future and technical considerations of gold wirebonding in semiconductor packaging – a technical review. *Microelectronics International*, 31(2), 121–128.

[6] Zhou, H., Zhang, Y., Cao, J., Su, C., Li, C., Chang, A., & An, B. (2023). Research Progress on Bonding Wire for Microelectronic Packaging. *Micromachines*, 14(432). https://doi.org/10.3390/mi14020432

[7] Guenther, T., Werum, K., Müller, E., Wolf, M., & Zimmermann, A. (2022). Characterization of Wire-Bonding on LDS Materials and HF-PCBs for High-Frequency Applications. *Journal of Manufacturing and Materials Processing*, *6*(1), 9. https://doi.org/10.3390/jmmp6010009

[8] Zulkifli, M. N., Abdullah, S., Othman, N. K., & Jalar, A. (2012). Some thoughts on bondability and strength of gold wire bonding. *Gold Bulletin*, 45(3), 115–125.

[9] Chen, K.-J., Hung, F.-Y., & Chang, C.-Y. (2019). A Study of the Sulfidation Behavior on Palladium-Coated Copper Wire with a Flash-Gold Layer (PCA) after Wire Bonding. *Electronics*, *8*(7), 792. https://doi.org/10.3390/electronics8070792

[10] Fan, J., Yuan, D., Du, J., Hou, T., Wang, F., Cao, J., … Zhang, Y. (2024). Influence of Pd-Layer Thickness on Bonding Reliability of Pd-Coated Cu Wire. *Micromachines*, *15*(7), 931–931. https://doi.org/10.3390/mi15070931

[11] Kim, H.-T., Lee, D.-B., Lim, K.-S., Lee, J.-H., Park, S., Oh, C.-M., & Yoon, J.-W. (2024). Impact of bonding methods and surface finishes on terminal-substrate reliability in EV power modules. *Journal of Materials Science Materials in Electronics*, *35*(23). https://doi.org/10.1007/s10854-024-13371-0

[12] Harman, G. (2010). *Wire Bonding in Microelectronics* (3rd ed.). New York, NY: McGraw-Hill.